Electronic Supplementary Material (ESI) for Physical Chemistry Chemical Physics.

Electronic Supplementary Information, (ESI): "Magnetic structure of β-$Co(OH)_2$ and the effect of spin-orientation"

Diego Hunt, Gastón Garbarino, José Alberto Rodríguez-Velamazán*, Valeria Ferrari, Matías Jobbagy, and Damian A. Scherlis*

E-mail: velamazan@ill.fr,damian@qi.fcen.uba.ar

Determination of the magnetic structure from the neutron diffraction data

Representation analysis as described by Bertaut has been used to obtain possible configurations of the magnetic structure compatible with this magnetic propagation vector and the P-3m1 space group of β-Co(OH)$_2$. The six irreducible representations Γ_1 to Γ_6 of the vector group G_k (little group) were calculated using the program BasIreps, included in the FullProf Suite.[1] Γ_1 to Γ_4 are one-dimensional, while Γ_5 and Γ_6 are two-dimensional and have an imaginary part. An analysis of the imaginary representations shows that they can be transformed in two two-dimensional physically irreducible representations. In the present case Γ_5 and Γ_6, which are imaginary and two-dimensional, can be transformed to real matrices (Γ_6 and Γ_3, respectively) by application of a unitary transformation (see Table S1).

Table 1: Physically irreducible representations of the space group P-3m1 for k =(0,0,0.5). The symmetry elements are written according to Seitzs notation. ($a = 0.5$ and $b = 0.866$)

	$1\|000$	$3^+_{00z}\|000$	$3^-_{00z}\|000$	$2_{xx0}\|000$	$2_{0y0}\|000$	
${}^p\Gamma_1$	1	1	1	1	1	
${}^p\Gamma_2$	1	1	1	-1	-1	
${}^p\Gamma_3$	$\begin{bmatrix}1 & 0\\ 0 & 1\end{bmatrix}$	$\begin{bmatrix}-a & b\\ -b & -a\end{bmatrix}$	$\begin{bmatrix}-a & -b\\ b & -a\end{bmatrix}$	$\begin{bmatrix}-a & -b\\ -b & a\end{bmatrix}$	$\begin{bmatrix}-a & b\\ b & a\end{bmatrix}$	
${}^p\Gamma_4$	1	1	1	1	1	
${}^p\Gamma_5$	1	1	1	-1	-1	
${}^p\Gamma_6$	$\begin{bmatrix}1 & 0\\ 0 & 1\end{bmatrix}$	$\begin{bmatrix}-a & b\\ -b & -a\end{bmatrix}$	$\begin{bmatrix}-a & -b\\ b & -a\end{bmatrix}$	$\begin{bmatrix}-a & -b\\ -b & a\end{bmatrix}$	$\begin{bmatrix}-a & b\\ b & a\end{bmatrix}$	
	$-1\|000$	$-3^+_{00z}\|000$	$-3^-_{00z}\|000$	$M_{x2xz}\|000$	$M_{x-xz}\|000$	$M_{2xxz}\|000$
${}^p\Gamma_1$	1	1	1	1	1	1
${}^p\Gamma_2$	1	1	1	-1	-1	-1
${}^p\Gamma_3$	$\begin{bmatrix}1 & 0\\ 0 & 1\end{bmatrix}$	$\begin{bmatrix}-a & b\\ -b & -a\end{bmatrix}$	$\begin{bmatrix}-a & -b\\ b & -a\end{bmatrix}$	$\begin{bmatrix}1 & 0\\ 0 & -1\end{bmatrix}$	$\begin{bmatrix}-a & -b\\ -b & a\end{bmatrix}$	$\begin{bmatrix}-a & b\\ b & a\end{bmatrix}$
${}^p\Gamma_4$	-1	-1	-1	-1	-1	-1
${}^p\Gamma_5$	-1	-1	-1	1	1	1
${}^p\Gamma_6$	$\begin{bmatrix}-1 & 0\\ 0 & -1\end{bmatrix}$	$\begin{bmatrix}a & -b\\ b & a\end{bmatrix}$	$\begin{bmatrix}a & b\\ -b & a\end{bmatrix}$	$\begin{bmatrix}-1 & 0\\ 0 & -1\end{bmatrix}$	$\begin{bmatrix}a & b\\ b & -a\end{bmatrix}$	$\begin{bmatrix}a & -b\\ -b & -a\end{bmatrix}$

The magnetic representation Γ_M for the magnetic site [1a Wyckoff position (0,0,0)] can be decomposed as a direct sum of the physical irreducible representations ${}^p\Gamma_2$ and ${}^p\Gamma_3$,

$$\Gamma_M(1a)={}^p\Gamma_2 \oplus {}^p\Gamma_3.$$

The magnetic structure can only be described by ${}^p\Gamma_2$, ${}^p\Gamma_3$ or a combination of both. In the case of ${}^p\Gamma_3$ the magnetic structure is constrained to be in the *ab*-plane (it should be noted that, in the present symmetry, all the orientations of the magnetic moments contained in the *ab* plane are equivalent), while ${}^p\Gamma_2$ gives a contribution strictly along the *c*-axis. These two configurations can be described from the set of basis vectors shown in the following table, showing the basis vectors of the two possible physical irreducible representations (${}^p\Gamma_2$ and ${}^p\Gamma_3$) for the site 1a (Space Group P-3m1, magnetic propagation vector k=(0,0,0.5)).

Table 2: Basis vectors of the two possible physical irreducible representations (${}^p\Gamma_2$ and ${}^p\Gamma_3$) for the site 1a (Space Group P-3m1, magnetic propagation vector k=(0,0,1/2)).

${}^p\Gamma_2$	(0	0	1)			
${}^p\Gamma_3$	(1	0	0)	(-3.4641	-6.9282	0)

The configuration with moments purely along *c* is discarded because it does not reproduce the experimental data. On the other hand, the main features of the magnetic diffraction pattern are well reproduced by the model with the magnetic moments parallel to the plane (Figure 5 of the main text in the current submission). The agreement can be further increased by introducing an out-of-plane component (that is, an admixture of both representations; Figure 5). The final refinement has been done using this model, with the magnetic moment described in spherical coordinates, maintaining the azimuth ϕ angle (orientation within the *ab* plane) fixed at an arbitrary direction as the only constraint (apart from the one imposed by the propagation vector k = (0,0, 0.5), which implies that Co(II) ions in adjacent planes are antiferromagnetically aligned.

Table 3: Experimental conditions and main parameters from the refinement of the powder neutron diffraction pattern of β-$Co(OH)_2$ at 3.5 K: Refined lattice parameters, fractional atomic coordinates, isotropic temperature factors, and reliability factors (see Ref. [19]). The space group is P-3m1(62) and the atoms are located at the following Wyckoff positions: Co at (1a) (0,0,0); O and H at (2d) (1/3, 2/3, z).

Formula	β-$Co(OH)_2$
T(K)	3.5
Inst.λ (Å)	D2B, 1.5966
Crystal System	Trigonal
Space Group Num.	P-3m1 (62)
a, b (Å)	3.18098(4)
c (Å)	4.63405(9)
α, β (°)	90
γ (°)	120
Vol ($\mathring{A}^3$)	40.918(3)
Z	1
Coordinates:	
z(O)	0.22727(49)
z(H)	0.42817(79)
Isotropic temperature factors:	
B(Co) ($\mathring{A}^2$)	0.206(74)
B(O) ($\mathring{A}^2$)	0.729(23)
B(H) ($\mathring{A}^2$)	2.875(52)
Co magnetic moment	
μ (μB)	2.22(3)
θ (°)(out of plane angle)	57.9(6)
R_B (%)	6.88
R_{Mag} (%)	13.5
χ^2	2.1

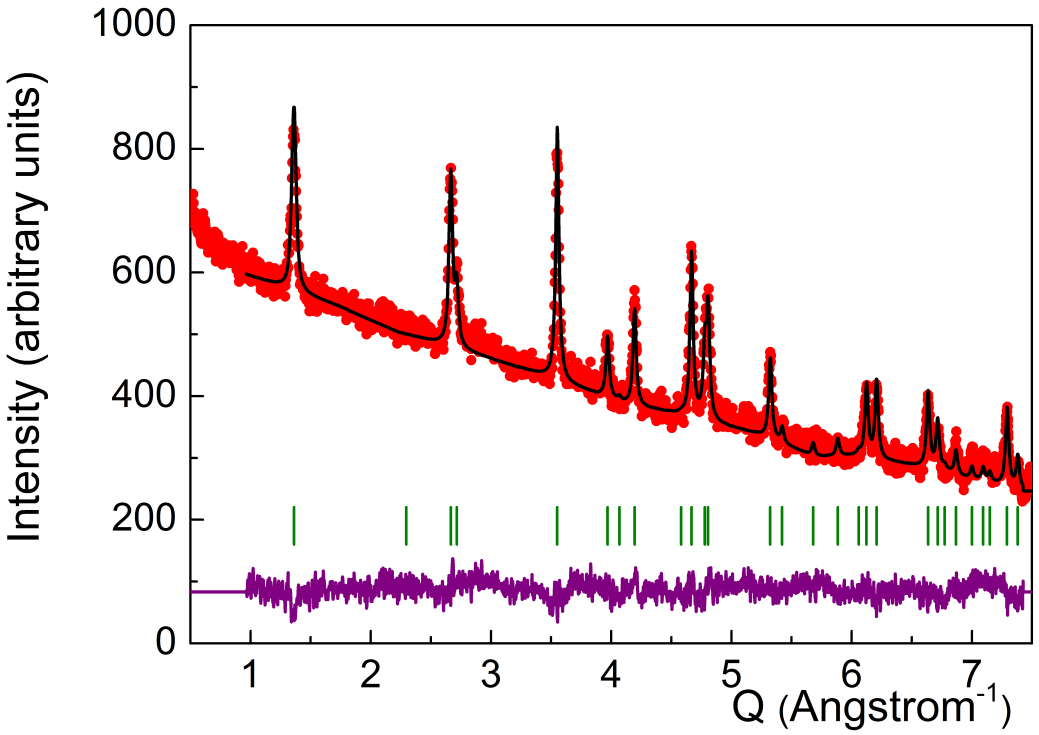

Figure S1. Experimental and calculated neutron diffraction patterns of β-Co(OH)$_2$ at room temperature. Data collected at D2B instrument with $\lambda = 1.5966$ Å. The red points and black line stand for experimental and calculated intensities, respectively. The difference is plotted at the bottom (purple line, shifted in vertical for clarity), and the bars indicate the positions of the Bragg reflections. The observed pattern well corresponds to the crystal structure of β-Co(OH)$_2$, with no evidence of impurities. Details of the refinement: Space group P-3m1(62); cell parameters $a = b =$ 3.1843(1) Å, $c = 4.6598(2)$ Å. The atoms are located at the following Wyckoff positions: Co at (1a) (0,0,0); O and H at (2d) (1/3, 2/3, z); and the refined atomic coordinates are: z(O) = 0.2198(7) and z(H) = 0. 4113 (21).

About the purity of the sample

The synthesis protocol, including a final step of mild drying of the washed sample, effectively prevents the oxidation of Co(II). Only after two months exposed to ambient oxygen and moisture conditions, the β-$Co(OH)_2$ powder develops incipient oxidation, evidenced by a pale brownish color instead of the inherent intense pink of the parent pure beta phase. Our preliminary stability test assessed by thermogravimetric analysis under oxygen rich atmosphere, displayed in the following figure, revealed that massive oxidation of $Co(OH)_2$ to Co_3O_4 starts at 150 °C, in agreement with the values reported by Sasaki group.[2]

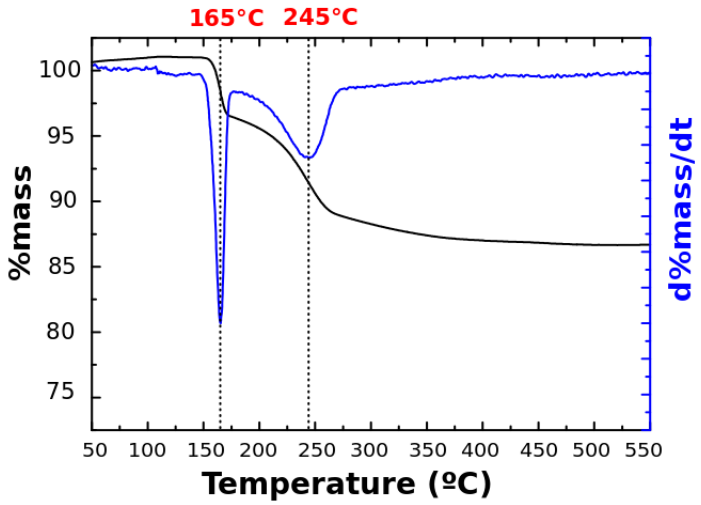

Figure S2

On the other hand, the three panels in Figure S3 compare the X ray diffraction patterns obtained from our sample, with the main reflections of the non-oriented β-$Co(OH)_2$ phase (orange), and with possible oxidation products,[3] as double layered hydroxides Co(II)-Co(III) (blue) and Co_3O_4 (red). Whereas all the main experimental reflexions obey to the β-$Co(OH)_2$ phase, in the last two panels, the main signals of these phases are different from the experimental pattern.

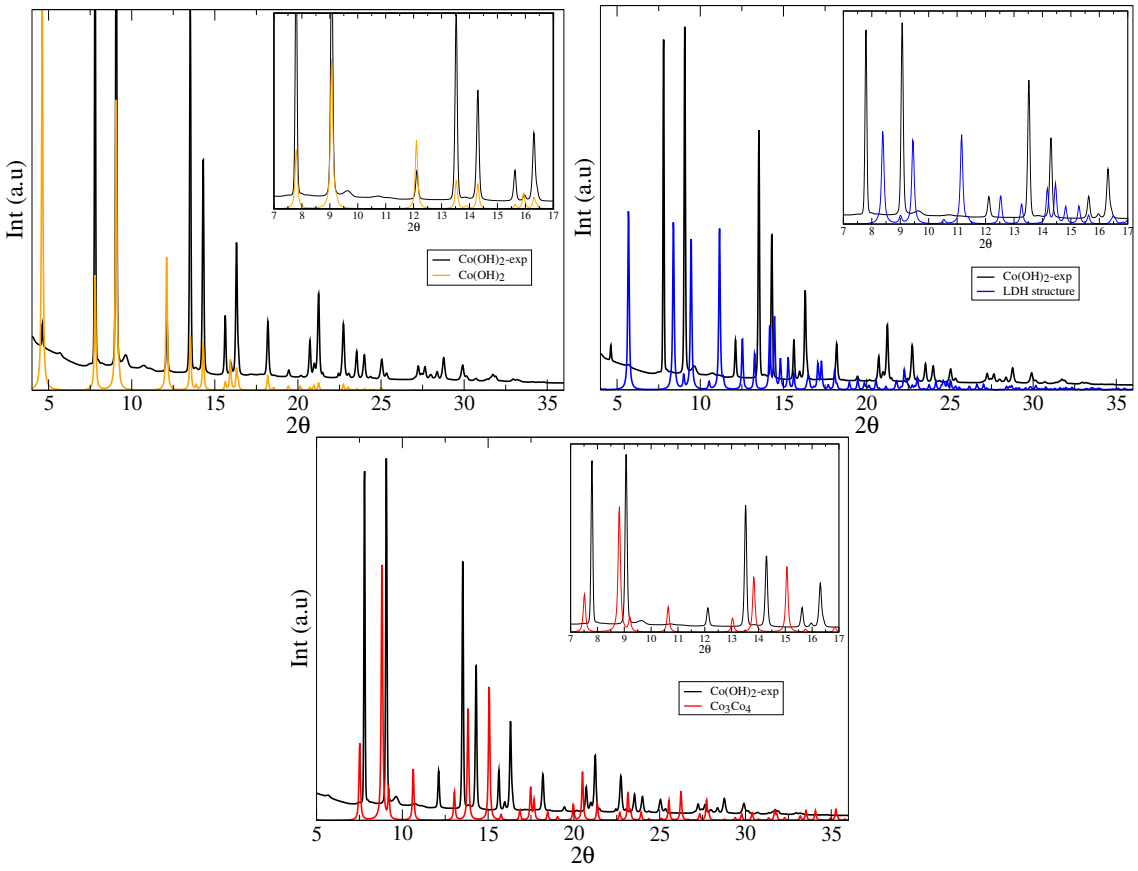

Figure S3

CIF files used to refine the structural data

To refine the data we departed from a structural model reported in the literature and in the databases. In the case of the icsd database, it is the file 88940 associated with the paper "The distortion of the hexagonal close packing of oxygen atoms in β-$Co(OH)_2$ compared to isotypic brucite-type structure.[4]

Assessment of spin-orbit interactions

Fully relativistic pseudopotentials within the LDA formalism were used to include spin-orbit interactions in a non-collinear setting.[5]

In this case, an energy cutoff of 50 and 400 Ry was used to expand the electronic wave

functions and the charge density, respectively, employing a 2×2×1 k-point mesh.

Discussion on the dimerization with the magnetic moment constrained to the *c*-axis

The Goodenough-Kanamori-Anderson rules establish the nature of the superexchange interactions between two ions bridged by a non-metallic ligand as a function of bond angle and orbital occupations.[6] A linear configuration favors strong overlaps and large splittings between the emerging molecular orbitals, leading to singlet or antiferromagnetic states. As the angle is reduced, the molecular orbitals tend to equalize and the triplet or ferromagnetic coupling is favored. Consistently, the Co-O-Co angle subtended between antiferromagnetic dimers in this lattice is 98.24°, whereas the angle between ferromagnetically coupled centers is 95.53°. The Co-O distance, on the other hand, remains practically invariant. It turns out that the spin state in the lattice can be explained through the superexchange interaction arising in a single dimeric CoO_2Co unit. The coupling between cobalt centers in this small model is antiferromagnetic for angles above 97°, becoming ferromagnetic below this value (see Figures S4 and S5). This trend is in quantitative agreement with the behavior reported for copper complexes containing the CuO_2Cu motif.[7,8]

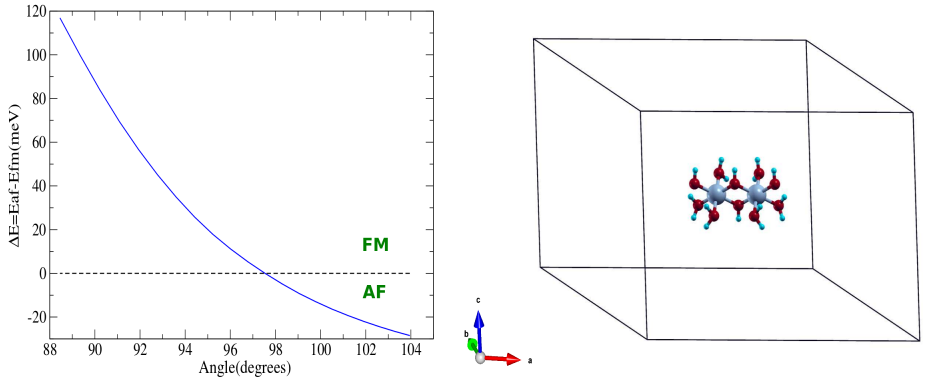

Figure S4. Energy difference between the AF and FM states as a function of the Co-O-Co angle, for the cobalt dinuclear complex bridged by two oxygen atoms represented on the right.

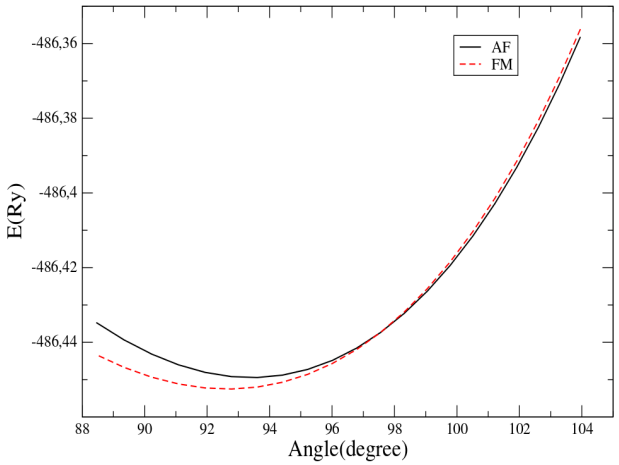

Figure S5. Total energies for the AF and FM states as a function of the Co-O-Co angle, for the cobalt dinuclear model depicted above. The coupling is antiferromagnetic for angles above 97°, becoming ferromagnetic below this value. This trend is in quantitative agreement with the behavior reported for copper dinuclear complexes containing the CuO_2Cu unit, where the ground state changes from a singlet to a triplet for angles below $\sim 98°$.[7,8] In the present model, on the other hand, the antiferromagnetic state turns out to be slightly more stable, presenting an optimized Co-O-Co angle of 92.5°. In the solid, where each oxygen atom bridges three metallic centers, the Co-O-Co angles are slightly increased. By breaking the symmetry, the lattice is able to accommodate one every two pairs of cobalt ions in a geometry suited for ferromagnetic coupling, retrieving in this way an additional exchange energy.

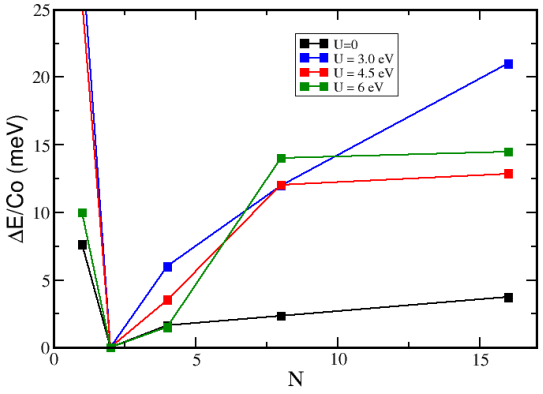

Figure S6. Relative energy computed with DFT and DFT+U as a function of the extension of the magnetically collinear domains, N, constraining the orientation of the magnetic moment on the c-axis. N=1 and N=16 represent respectively the regular AF and FM arrangements. The most favorable configuration involves spin dimers (N=2).

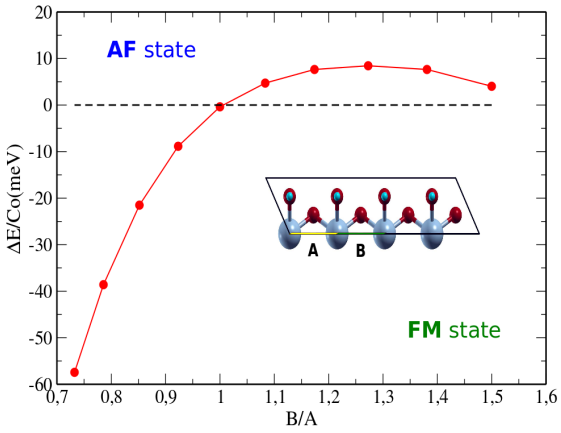

Figure S7. Magnetic phase diagram for an assymetric unit cell containing 4 cobalt ions, as shown in the inset. The vertical axis represents the energy difference $\Delta E = E_{FM} - E_{AF}$ as a function of the bond length ratio, B/A. The AF state is the dimerized configuration with parallel spins separated by a distance A and antiparallel spins separated by a distance B. The minimum energy configuration corresponds to B/A=1.03, inside the AF region of the diagram.

References

(1) Rodríguez-Carvajal, J. *Phys. B (Amsterdam, Neth.)* **1993**, *192*, 55–56.

(2) Liu, Z.; Ma, R.; Osada, M.; Takada, K.; Sasaki, T. *J. Am. Chem. Soc.* **2005**, *127*, 13869–13874.

(3) Ma, R.; Takada, K.; Fukuda, K.; Iyi, N.; Bando, Y.; Sasaki, T. *Angew.Chem.Int.Ed.* **2008**, *47*, 86–89.

(4) Pertlik, F. *Monatsh. Chem.* **1999**, *130(9)*, 1083–1088.

(5) Dal Corso, A.; Mosca Conte, A. *Phys. Rev. B* **2005**, *71*, 115106.

(6) Goodenough, J. *Magnetism and the Chemical Bond*; Interscience Publisher: New York, 1963.

(7) Hay, P.; Thibeault, J.; Hoffmann, R. *J. Am. Chem. Soc.* **1975**, *97*, 4884–4899.

(8) Hatfield, W. *Inorg. Chem.* **1983**, *22*, 833–837.